



this context, methods designed for unified representations have been studied with the goal of reducing computational complexity. Moment representations have been shown to be effective in significantly reducing the size of ensemble system dynamics [17]. Moment dynamics are essentially a spectral approximation of the ensemble in Hilbert space, with the spectral accuracy property that ensures exponential convergence to the continuum state with increasing approximation order. This representation enables design of control sequences for ensemble systems in a space of greatly reduced dimension without significant loss of precision [18].

In this paper, we revisit the problem of matter-wave splitting involving a Bose-Einstein condensate (BEC) in a standing light wave potential [15]. We consider optical standing-wave beam splitters for which the effect of an optical pulse is subject to experimental inhomogeneities, which we represent by an uncertain factor applied to the light wave amplitude envelope. This results in an ensemble system, whose evolution we describe using the Legendre moment dynamics. In this reduced space, we design pulse sequences that transfer the state of the ensemble to a desired set-point, and evaluate the improved fidelity of the BEC momentum transfer within the quantum state space.

This project is organized as follows. In Section II, we derive the mathematical representation of the BEC-splitting system from the Schrödinger's equation, and characterize the source of inhomogeneity. In Section III, we then reproduce a state-of-the-art method of using square pulse sequences for optical splitting of matter-waves without compensating for inherent inhomogeneity [2]. In Section IV, we describe the Legendre moment representation of the BEC splitting dynamics, our proposed method for light pulse design within the moment space, and the resulting optimal control formulation. We present the computed optimal controls and simulations of the resulting momentum transfers in Section V for several diffraction orders, which show a significant improvement in fidelity with respect to the benchmark method. Finally, we conclude in Section VI.

## II. ENSEMBLE SYSTEM FOR BEC SPLITTING

We consider a dilute BEC composed of an initially stationary population of atoms, which is exposed to a standing-wave light field that excites the cluster of particles with similar, yet distinct intensities. The governing dynamics for this system are described by a one-dimensional Schrödinger's equation for a single atom. Inhomogeneity in the light beam is represented by a multiplicative parameter  $\varepsilon$  that scales the light shift potential amplitude  $\Omega(t)$ , which leads to a wave function

$$i\dot{\psi}(x, t, \varepsilon) = \left( -\frac{\hbar}{2m} \frac{d^2}{dx^2} + \varepsilon \Omega(t) \cos(2k_0 x) \right) \psi(x, t, \varepsilon). \quad (1)$$

The time-dependent parameter  $\Omega(t)$  serves as the control input to the system available to the experimenter, and  $k_0$  is the wave vector of the light field. We suppose that  $\varepsilon \in K$  is the physical representation of the unequal influence of the control pulse on individual atoms in the BEC sample,

where  $K \equiv [1 - \delta, 1 + \delta]$  is a compact interval. Each atomic particle can be viewed as corresponding to a unique  $\varepsilon$ , which permits us to use this parameter as an identifier to index the individual systems in the sample.

Equation (1) can be further developed into a sequence of coupled Raman-Nath equations by describing the wave function within the Bloch basis. The resulting differential equations dictate the time evolution of the beam-splitter state populations (represented by ground state  $C_0$ , and symmetric and anti-symmetric superpositions of momentum states  $C_{2n}^+$  and  $C_{2n}^-$ , for  $n = 0, 1, 2, \dots$ ) and the manner in which these interact. This infinite-dimensional system of ordinary differential equations (ODEs) is [15]

$$i\dot{C}_{2n}(k, t) = \frac{\hbar}{2m} (2nk_0 + k)^2 C_{2n}(k, t) + \frac{\varepsilon \Omega(t)}{2} [C_{2n-2}(k, t) + C_{2n+2}(k, t)]. \quad (2)$$

We make several assumptions in order to further simplify these infinite-dimensional Raman-Nath equations:

- The dependence on parameter  $k$  is dropped by assuming the system to be narrowly distributed around the value of  $k = 0$ .
- The coupling of the states  $C_0$  and  $C_{2n}^+$  with their anti-symmetric counterparts  $C_{2n}^-$  is considered negligible by assuming that  $k \ll k_0$ .
- A value  $N^+$  is defined such that all levels above  $C_{2N^+}^+$  are permanently unpopulated. This is achievable by assuming that all atoms are at rest at the beginning and that  $\Omega(t)/2 \ll (2N^+)^2 \hbar k_0^2 / 2m = (2N^+)^2 \omega_r$ , where  $\omega_r$  is the photon recoil frequency.

This mathematical setting has been developed in a variety of previous studies on matter-wave splitting techniques [19], [15], [2]. The resulting state-space system is described by

$$\frac{d}{dt} \begin{bmatrix} C_0(t, \varepsilon) \\ C_2^+(t, \varepsilon) \\ \vdots \\ C_{2N^+}^+(t, \varepsilon) \end{bmatrix} = -i\omega_r A(\varepsilon, \Omega(t)) \begin{bmatrix} C_0(t, \varepsilon) \\ C_2^+(t, \varepsilon) \\ \vdots \\ C_{2N^+}^+(t, \varepsilon) \end{bmatrix}, \quad (3)$$

where  $A(t, \varepsilon)$  is a real  $(N^+ + 1 \times N^+ + 1)$  symmetric matrix defined by

$$A(\varepsilon, \Omega(t)) = \begin{bmatrix} 0 & 0 & 0 & \dots & 0 \\ 0 & 4 & 0 & \dots & 0 \\ 0 & 0 & 16 & \dots & 0 \\ \vdots & \vdots & \vdots & \ddots & \vdots \\ 0 & 0 & 0 & \dots & (2N^+)^2 \end{bmatrix} + \frac{\varepsilon \Omega(t)}{2\omega_r} \begin{bmatrix} 0 & \sqrt{2} & 0 & 0 & \dots & 0 \\ \sqrt{2} & 0 & 1 & 0 & \dots & 0 \\ 0 & 1 & 0 & 1 & \dots & 0 \\ 0 & 0 & 1 & 0 & \ddots & \vdots \\ \vdots & \vdots & \vdots & \ddots & \ddots & 1 \\ 0 & 0 & 0 & \dots & 1 & 0 \end{bmatrix}. \quad (4)$$

For the system in Equations (3)-(4), we define the state vector  $C^+ = [C_0, C_2^+, \dots, C_{2N^+}^+] \in \mathbb{C}^{N^++1}$ . A goal of this study is to enable constrained optimization approaches for pulse design, for which the complex dynamics in Equations (3)-(4) must be converted to a real-valued system. We thus define  $C_{\mathbb{R}}^+ \in \mathbb{R}^{2(N^++1)}$  such that  $C_{\mathbb{R}}^+ = [C_{0,Re}, C_{0,Im}, C_{2,Re}^+, C_{2,Im}^+, \dots, C_{2N^+,Re}^+, C_{2N^+,Im}^+]$ , in terms of which the time evolution dynamics are

$$\frac{d}{dt} C_{\mathbb{R}}^+ = \omega_r A(\varepsilon, \Omega(t)) \otimes \begin{bmatrix} 0 & -1 \\ 1 & 0 \end{bmatrix} C_{\mathbb{R}}^+, \quad (5)$$

where  $\otimes$  is the Kronecker product.

In the above representation, the momentum dynamics for each atom are truncated to a finite-dimensional quantum system of  $N^++1$  levels. Nonetheless, due to the presence of parameter  $\varepsilon$ , there is a collection of infinitely many systems that must be steered simultaneously by a common control input. Next, we examine methods to design control pulses for momentum transfer of the system (5) that are invariant to a continuum of values of the uncertain parameter  $\varepsilon$ .

### III. SPLITTING MATTER USING SQUARE PULSES

A previously proposed approach for splitting matter waves uses a sequence of two square pulses for the envelope of an optical input that is applied to a dilute BEC in a standing light wave potential. The approach has been shown to have a high degree of precision in simulation, and can be applied in practice [15], [20]. The drawback of this method is its use of a single nominal system to define the dynamic response of each atom in the BEC to the optical pulse, so there is no compensation for inherent inhomogeneities. We describe the square-pulse design procedure below, and extend the original methodology with pulses of equal amplitude to the design of sequences of pulses with different amplitudes, which has been shown to enable higher fidelity [2].

#### A. Square optical pulse design for a single system

The square pulse optimal design problem involves the optimization of five parameters, which are illustrated in Figure 1. The decision variables are the time durations  $\tau_1$  and  $\tau_3$  of the pulses, the time interval  $\tau_2$  between the pulses, and the amplitudes  $\Omega_1$  and  $\Omega_2$  of the first and second square pulses, respectively. These parameters determine the final state of the system after the pulse is employed, which can be described by continuously applying the variation of parameters formula to Equation (3). The state at the terminal time  $\tau_{ps} = \tau_1 + \tau_2 + \tau_3$  of the pulse sequence is

$$\begin{aligned} C^+(\tau_{ps}, \varepsilon) &= e^{-i\omega_r \tau_3 A_3} e^{-i\omega_r \tau_2 A_2} e^{-i\omega_r \tau_1 A_1} C^+(0, \varepsilon) \\ \text{s.t. } A_1 &= A(\varepsilon, \Omega_1), A_2 = A(\varepsilon, 0), \\ A_3 &= A(\varepsilon, \Omega_2), \tau_{ps} = \tau_1 + \tau_2 + \tau_3. \end{aligned} \quad (6)$$

In the baseline scenario, we suppose that  $\varepsilon = 1$ . The control design goal is to transfer the momentum state of the sample from an initial rest state  $C^+(0) = [1, 0, 0, \dots, 0]^T$  to a final desired state  $C_f^+$ . This desired state is typically defined with respect to the  $L^2$ -norm (in quantum momentum space),

in which an energy level  $2n$  is reached at the end of the sequence of pulses, so that  $\|C_{f,2n}^+\|_2 = \|C_f^+\|_2 = 1$ . For this control task, the optimization problem can be formulated as

$$\begin{aligned} \min_{\Omega_1, \Omega_2, \tau_1, \tau_2, \tau_3} & \quad \| |C_f^+| - |C^+(\tau_{ps}, 1)| \|_2 \text{ as in Eq.(6)} \\ \text{s.t.} & \quad \text{Dynamics in Equations (4)-(5).} \end{aligned} \quad (7)$$

The procedure described above follows the original methodology for the design of square pulse sequences for matter wave splitting. Because a nominal parameter  $\varepsilon$  is used, the approach does not account for non-uniform influence of the pulse on the dynamical behavior of individual atoms in the BEC, and we expect that control performance is not robust to values of  $\varepsilon$  away from unity. We extend the formulation below by adding dynamic constraints for samples of  $\varepsilon \in K$  as an attempt to account for the dynamics of an ensemble of atoms that are affected inhomogeneously by the applied pulse sequence.

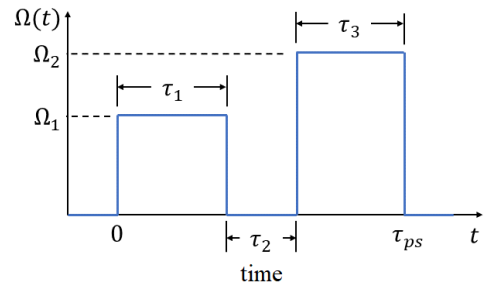


Fig. 1: Illustration of a square pulse sequence control  $\Omega(t)$  and parameters.

#### B. Square optical pulse design for ensemble system

We extend the optimization problem (7) defined in the previous section to account for multiple values of  $\varepsilon$ . Because it is intractable to define dynamic constraints for each system in an infinite-dimensional ensemble, we define an objective function as a summation of minimum  $L_2$  norm objectives for  $m$  values of  $\varepsilon$  sampled directly from the parameter domain  $K$ . The optimization is conducted subject to dynamic constraints for each of the same  $m$  values of  $\varepsilon$ .

We define the finite collection of parameters  $\varepsilon_{1:m} = \{\varepsilon_1, \varepsilon_2, \dots, \varepsilon_m\} \subset K$ , such that  $\varepsilon_1 = \arg \min_K \varepsilon$ ,  $\varepsilon_m = \arg \max_K \varepsilon$ , with intermediate samples uniformly spaced on  $[\varepsilon_1, \varepsilon_m]$ . The simultaneous optimization for all systems indexed by  $i \in \{1, 2, \dots, m\}$  is formulated as

$$\begin{aligned} \min_{\Omega_1, \Omega_2, \tau_1, \tau_2, \tau_3} & \quad \sum_{i=1}^m \| |C_f^+| - |C^+(\tau_{ps}, \varepsilon_i)| \|_2 \\ \text{s.t.} & \quad \text{Dynamics in Equations (4)-(5) } \varepsilon = \varepsilon_i, \\ & \quad \forall i = 1, \dots, m. \end{aligned} \quad (8)$$

The control pulse sequences that are obtained by solving the optimization problems (7) and (8) will be used as benchmarks in Section V to demonstrate the performance improvement gained by way of the proposed moment dynamics method.

#### IV. CONSTRAINED ENSEMBLE PROBLEM USING MOMENT DYNAMICS

We present a novel approach to improve light pulse design methods for matter-wave splitting by compensating for the inherent inhomogeneities that are present in physical systems. In this section, we derive a polynomial moment based representation of the ensemble dynamics of the matter wave splitting process, and formulate an ensemble control problem for optimal state transfer of a BEC sample in momentum space.

The polynomial moment ensemble approach has been applied recently to design open-loop controls to transfer ensemble systems between initial and target states in Hilbert space, demonstrating low terminal state error [17], [21], [9]. The method enables a control problem for an infinite-dimensional continuum to be reduced to a finite-dimensional control problem by transforming the state space using a polynomial approximation that can then be truncated at a sufficiently high order. The transformation facilitates the design of a single control input that steers the moments to a desired representation in the spectral moment space, which is equivalent to steering each individual element of the ensemble to its target in the state space [14].

The moment-based approach for ensemble control systems can be defined using any basis from a diverse collection of orthogonal polynomials. For this project, we have chosen to use Legendre polynomials as the basis of the moment system, because this particular basis has desirable properties for approximation of continuous functions on compact intervals [18]. This representation has also been used previously for controlling the Bloch equations that represent a two-level quantum system in the context of NMR [14].

##### A. Moment Systems using Legendre Polynomials

The concept of moment space representation begins with a function defined within a separable Hilbert space  $\mathcal{H}$ . If a basis  $\{|\psi_k\rangle : k \in \mathbb{N}^d\}$  can be defined (for simplicity, we will use  $d = 1$ ), then the moment of order  $k$  for a function  $x(t)$  can be defined by

$$m_k(t) = \langle x(t) | \psi_k \rangle. \quad (9)$$

For an ensemble of systems indexed by a parameter varying in the compact interval  $K = [-1, 1]$ , it is possible to obtain the equivalent Legendre moments by using the respective orthogonal polynomials  $P_k(\varepsilon)$ , obtained using the recursive relation given, after normalization, by

$$\varepsilon P_k = c_{k-1} P_{k-1} + c_k P_{k+1}, \quad (10)$$

where  $P_0(\varepsilon) = 1/\sqrt{2}$ ,  $P_1(\varepsilon) = \sqrt{3/2}\varepsilon$ , ..., are the normalized Legendre polynomials and  $c_k = (k+1)/\sqrt{(2k+1)(2k+3)}$ . In this setting, the Legendre moment of order  $k$  for the vector of quantum states  $C^+(t, \varepsilon)$  is defined by

$$m_k(t) = \langle C^+(t), P_k \rangle = \int_{-1}^1 C^+(t, \varepsilon) P_k(\varepsilon) d\varepsilon. \quad (11)$$

Taking the time derivative of Equation (11) yields the equivalent moment dynamics of the ensemble system. The use of the Legendre polynomial basis to define moment spaces was shown to possess a variety of advantages for representing ensemble systems. For instance, the Legendre polynomials form an orthogonal basis on the Hilbert space  $\mathcal{H}$ , which induces an isometry between the moment space and the quantum ensemble system. The preservation of metrics through this transformation has advantages for defining tractable optimization formulations to represent optimal control problems for ensemble systems. The recursive relation in Equation (10) also enables the description of moment dynamics defined by bounded operators. Finally, the control profile is preserved with transformation between the moment space and state space, so that practical control design is possible using the moment dynamics method.

##### B. BEC Splitting in the Moment Space

We apply the transformation in Equation (11) to the time-evolution model for the quantum system described by Equations (4)-(5) to obtain the dynamics of the corresponding Legendre moments. The quantum ensemble system is defined for the ensemble parameter  $\varepsilon \in K = [1 - \delta, 1 + \delta]$ , such that  $\delta \in (0, 1)$ , which is a different compact interval than the domain of the Legendre polynomial basis. Therefore, we define a parameter  $\varepsilon^*$  such that  $\varepsilon = 1 + \delta\varepsilon^*$ , meaning that  $\varepsilon^* \in [-1, 1]$ , and the moments are calculated using the Hilbert space related to parameter  $\varepsilon^*$ . In this setting, the moment dynamics for  $m(t) = [m_0(t), m_1(t), \dots, m_{N-1}(t)]$  are described by

$$\begin{aligned} \dot{m}(t) = \omega_r \left[ I(N) \otimes A(1, \Omega(t)) \otimes \begin{bmatrix} 0 & -1 \\ 1 & 0 \end{bmatrix} \right. \\ \left. + \mathcal{C}(N) \otimes (A(\delta, \Omega(t)) - A(\delta, 0)) \otimes \begin{bmatrix} 0 & -1 \\ 1 & 0 \end{bmatrix} \right] \cdot m(t), \end{aligned} \quad (12)$$

where  $I(N)$  is an identity matrix of dimension  $N \times N$  and  $\mathcal{C}(N)$  is defined by

$$\mathcal{C}(N) = \begin{bmatrix} 0 & c_0 & & & \\ c_0 & 0 & c_1 & & \\ & c_1 & \ddots & \ddots & \\ & & \ddots & 0 & c_{N-2} \\ & & & c_{N-2} & 0 \end{bmatrix}. \quad (13)$$

With the Legendre moment dynamics as defined in Equation (12), we can state an optimization problem that approximates the optimal control problem for the ensemble in state-space. The orthogonality property of the Legendre polynomial basis defines an isometry between the two studied spaces, which enables a metric to be used to specify an objective for the optimization problem. Moreover, it is also possible to include inequality constraints in the optimization problem, which we will apply in the control design. We are interested specifically in enforcing limits on the absolute amplitude and the rate of change of the control function.

Specifying the final state in moment space requires an additional reformulation. In the state-space, the optimization objective is defined in terms of the absolute value of the final state, as in Equation (7). To express an objective function that depends on the state of an ensemble system, we formulate the objective in moment space. To that end, we minimize the magnitude of the undesired energy levels by aiming to nullify their states, i.e.,  $\|C_f^+ \circ (\mathbf{1}_{2(N+1)} - e_{n+1} \otimes \mathbf{1}_2)\|_2 = 0$ . The resulting optimization problem in moment space is

$$\begin{aligned} \min_{\Omega(t)} \quad & \|m(T) \circ [\mathbf{1}_N \otimes (\mathbf{1}_{2(N+1)} - e_{n+1} \otimes \mathbf{1}_2)]\|_2 \\ \text{s.t.} \quad & \text{Dynamics in Equations (12)-(13),} \\ & \Omega_{min} \leq \Omega(t) \leq \Omega_{max}, \\ & \Delta\Omega_{min} \leq \dot{\Omega}(t) \leq \Delta\Omega_{max}, \end{aligned} \quad (14)$$

where  $T$  is a predefined time horizon, similar to the parameter  $\tau_{ps}$  used in problems (7) and (8).

## V. CONTROL SYNTHESIS RESULTS

The Legendre moments method for matter-wave splitting ensemble control design is evaluated by comparing its performance with that of the square pulse sequence method. We first compare the Legendre moments approach with the controls obtained by solving the problem in Equation (7). A similar comparison is then done with respect to controls obtained by solving the problem in Equation (8), which seeks to account for variation in  $\varepsilon$  by sampling values directly in the ensemble space  $K$ . To compare the performance of the various control designs in achieving the goal of transferring the ensemble to the target in Hilbert space on  $K$ , we define an index  $I_e$  based on the objective function for the pulse design in the quantum state space. This performance index, which we seek to minimize, is defined as

$$I_e = \int_{1-\delta}^{1+\delta} \| |C_f^+| - |C^+(T, \varepsilon)| \|_2 d\varepsilon. \quad (15)$$

### A. Computational Approach

We solve the optimal control problem (14) using a general iterative scheme for computing optimal control inputs for nonlinear systems [22]. For a general continuous-time nonlinear control system of the form  $\dot{x}(t) = f(x(t), u(t))$ , where  $x(t)$  and  $u(t)$  are state and control vectors, respectively, a zero-order hold assumption is used to define the evolution of the system using a piece-wise constant control input. Beyond using a traditional first-order discretization and linearization, we use an approach that takes advantage of a higher-order Taylor series expansion to accurately represent linearization of nonlinear dynamics and their Jacobian at each iteration [23]. Beginning with an initial guess of the control function, the algorithm solves an approximation of the optimization problem in (14) to yield the optimal vector  $\Delta U$  of time-discretized variations in the control input that improves the objective value. This results in a sequence of quadratic programs, which, though each can be efficiently solved, require highly complex algebraic formulation of the dynamics in

Equations (12)-(13) when truncated at a high momentum level  $N^+$  and sufficiently high polynomial moment order to represent the quantum and ensemble dynamics in their respective Hilbert spaces. In contrast to previous applications of this approach to the control of quantum ensemble systems [18], the size and complexity of the dynamics examined here requires the iterative use of symbolic algebra to compute the Taylor expansion of the nonlinear dynamics, which becomes extremely complex.

Once the moment dynamics and the respective symbolic expressions are obtained, the pulse is designed by the iterative application of quadratic programming to solve the optimization problem in Equation (14). To apply the methodology defined in [23], the time domain  $[0, T]$  is finely discretized by using a small time step. We use a nominal value of  $\Delta t = 0.001$  over a total time horizon of  $T = 3$ , and this results in a total of 3000 variables and 12000 constraints for optimizing the variation  $\Delta U \in \mathbb{R}^{3000}$  that is added to the control function at each iteration. The same momentum level truncation at  $N^+ = 9$  and moment order  $N = 20$  are used in all of the computations.

---

### Algorithm 1 Iterative Moment Pulse Design Algorithm

---

**Require:**  $n$ , Initial pulse guess  $U$ , Moment dynamics  $M(t, m(t), u(t))$ , number of time steps  $N_{steps}$ ,  $\lambda$ ,  $f(m(t)) = m(t) \circ [\mathbf{1}_N \otimes (\mathbf{1}_{2(N+1)} - e_{n+1} \otimes \mathbf{1}_2)]$   
**Ensure:** Cost Function in Equation 14  $\leq$  **Tolerance**

- 1: **while**  $\|f(m(T))\| \geq$  **Tolerance** **do**
- 2:    $m(0), m(\Delta t), \dots, m(T) \leftarrow F(t, m(t), U)$
- 3:    $i \leftarrow 1$
- 4:   **while**  $i \leq N_{steps}$  **do**
- 5:      $A_i \leftarrow \frac{\partial}{\partial m} F((i)\Delta t, m((i)\Delta t), U_{i+1})$
- 6:      $B_i \leftarrow \frac{\partial}{\partial U} F((i)\Delta t, m((i)\Delta t), U_{i+1})$
- 7:      $i \leftarrow i + 1$
- 8:   **end while**
- 9:    $H \leftarrow [A_{N_{steps}} \dots A_2 B_1 | A_{N_{steps}-1} \dots A_3 B_2 | \dots$   
 $\quad | A_{N_{steps}} B_{N_{steps}-1} | B_{N_{steps}}]$
- 10:    $\Delta U \leftarrow \min_{\Delta U} \Delta U^T (H^T H + \lambda I) \Delta U$   
 $\quad + f(m(T))^T H \Delta U$
- 11:    $U \leftarrow U + \Delta U$
- 12: **end while**

---

The computational procedure used to synthesize ensemble controls is described in Algorithm 1, in which a cost function is iteratively reduced until a desired error tolerance is reached. The methodology can be described as consisting of three stages: (1) propagation of moment states using the current control profile; (2) linearization of time-localized dynamics; (3) and an update of the control profile. Both the propagation of moment states and respective linearizations are performed using a Taylor series expansion of higher order over the symbolic expression that represents the dynamics in Equation (12). This approach is adopted for improved precision in the linearized approximation defined by the set of matrices  $A_k$  and  $B_k$ , which are coupled in a matrix  $H$ , used to estimate the variation of the moment state at the final

time step. The optimization problem can be represented using a quadratic program with a quadratic objective function and linear constraints, which we solve using a quadratic programming solver. This function has a penalty term scaled using a parameter  $\lambda$ , which is used in order to avoid high variations in the defined control variation  $\Delta U$ , which would invalidate previously obtained linearized transformations. The related code is developed and executed on MATLAB<sup>TM</sup>, version R2023a.

In the following computational studies, the constraint bound values defined in Equation (14) are set to  $\Omega_{max} = 100$ ,  $\Delta\Omega_{min} = -500s^{-1}$ , and  $\Delta\Omega_{max} = 500s^{-1}$ . We examine control designs for various target states in momentum space with real controls where  $\Omega_{min} = -100$ , as well as with strictly non-negative real-valued control functions where  $\Omega_{min} = 0$ . Our computational results are described in the following section. Table I contains a list of control synthesis problems specified by different values of parameters  $n$  and  $\Delta\Omega_{min}$ , and the resulting time required to compute the ensemble controls. We observe that the computation time is affected by the increase in complexity required to achieve a higher momentum level  $n$ . All simulations were performed on a 2023 MacBook Pro with Apple(R) M2 Pro Processor at 3.4 GHz and 16GB of memory.

TABLE I: Computation times for moment pulse design.

$n$ in $C_f^+$	$\Delta\Omega_{min}$	Computation time (s)
1	0	866.4169
2	0	827.9643
3	0	1079.8969
4	0	1039.5165
1	-100	700.5696
2	-100	845.3960
3	-100	1001.5283
4	-100	1088.8991

### B. Moment Ensemble and Square Pulse Design

To demonstrate the performance improvement of the Legendre moment dynamics method with respect to the square pulse sequence obtained by solving problem (7), we compare controls computed for an ensemble defined by  $\delta = 0.1$ . The square pulses are designed using a maximum momentum level  $N^+ = 24$ , and the parameters that define the optimal pulses for target momentum states  $n = 1, 2, 3, 4$  are given in Table II. For control synthesis using the proposed moment ensemble method, we use a moment order  $N = 20$  and truncate the momentum level at  $N^+ = 9$ . The resulting controls are validated by applying them to simulations of the entire ensemble with  $\varepsilon \in [1 - \delta, 1 + \delta]$  with the momentum levels truncated above  $N^+ = 24$ .

TABLE II: Optimal square pulse design parameters.

$n$	$\Omega_1/\omega_r$	$\Omega_2/\omega_r$	$\omega_r\tau_1$	$\omega_r\tau_2$	$\omega_r\tau_3$
1	3.9865	2.2849	0.4744	0.9427	0.4181
2	13.0036	9.5440	1.000	0.7190	1.000
3	32.4012	34.7591	0.1905	0.5523	0.1913
4	41.4215	41.4263	1.2653	0.8002	1.9952

The real-valued and positive ensemble controls and terminal state error functions for the ensemble controls and

square pulse sequences are compared in Figure 2 for target momentum levels  $n = 1, 2, 3$ , and 4. The square pulse sequence performs as expected in each case, with error that is negligible at the nominal value of  $\varepsilon = 1$ , but which quickly increases as  $\varepsilon$  diverges from unity. In contrast, we see that the terminal state error for the simulation in which the controls obtained by solving problem (14) are applied to the ensemble remains quite low for all values of the ensemble parameter  $\varepsilon \in [0.9, 1.1]$  for target momentum levels  $n = 1, 2, 3$ , and still shows a significant performance advantage in the case of a target state  $C_f^+ = C_{f,2n}^+$  with  $n = 4$ .

The proposed method shows clear improvement with respect to all tested square pulse sequences in overall performance for momentum transfer of the ensemble of systems for positively-constrained controls as well as real-valued ones. Observe that the amplitude and variation of the controls obtained for  $n = 4$  are greater than for the lower valued momentum state targets, which can be explained by the need to manipulate higher frequency dynamics. Indeed, the constraints on amplitude and variation for control function are binding at many times during the optimization horizon, which necessarily limits the degree to which the algorithm can meet the optimization objective. There are inherent trade-offs between the constraint bound values, the optimization horizon, and the complexity of the control task, which we have illustrated here.

The performance achieved by the proposed method is quantified in Table III, in which the index  $I_e$  defined in Equation (15) is given for the square pulse controls and the positive and real valued ensemble controls as shown in Figure 2, for which the index values are denoted by  $I_{e,sp}$ ,  $I_{e,+}$  and  $I_{e,\mathbb{R}}$ , respectively. As seen in the top row of Figure 2, the results in Table III show that the positive valued ensemble controls result in a significant decrease in terminal error with respect to the square pulse sequence, and the real-valued ensemble controls are even better. We note that in practice, the control represents the amplitude envelope of an optical pulse, so  $\Omega(t)$  must remain positive in the present setting. Reformulation of the Raman-Nath equations and adjustment of the experimental setting may enable real-valued control inputs, however.

TABLE III: Performance results for moment ensemble controls for  $\delta = 0.1$ .

$n$	$I_{e,sp}$	$I_{e,+}$	$I_{e,\mathbb{R}}$
1	0.0141	0.0021	0.0004
2	0.0579	0.0012	0.0004
3	0.0515	0.0030	0.0006
4	0.1768	0.0608	0.0260

### C. Moment Ensemble and Ensemble Square Pulse Design

We also compare the ensemble control method to the square pulse controls obtained by solving the optimization problem in Equation (8). The comparison is made for three control design cases. First, the target state is  $n = 1$  with  $\delta = 0.1$ ; the second case has target state  $n = 4$  with  $\delta = 0.1$ ; and the third aims for  $n = 1$  with  $\delta = 0.4$ . The parameter values obtained by solving the square pulse design problem (8)

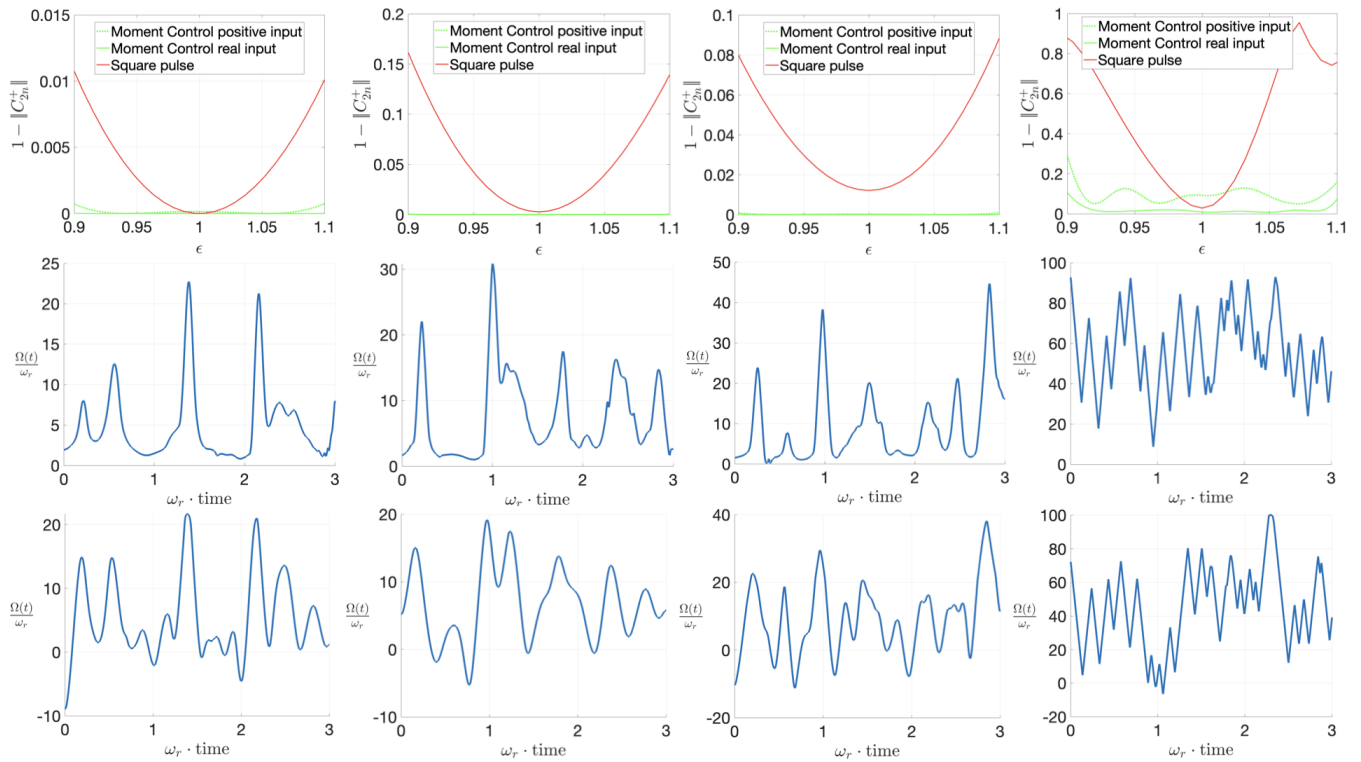


Fig. 2: Comparison of the performance of optimal square pulse sequences with moment ensemble controls. For all target states, we design for  $\delta = 0.1$ , and use a time horizon of  $T = 3$ . The desired momentum levels for these computations are (from left to right)  $C_2^+$ ,  $C_4^+$ ,  $C_6^+$ , and  $C_8^+$ . The plots show (from top to bottom): the final error achieved for the square pulse and the moment ensemble method as a function of the ensemble parameter  $\epsilon$ ; the optimal control function for strictly non-negative values of  $\Omega(t)$ ; and the optimal control when allowing real-valued inputs. Note that the skew-rate limit is binding in the control solutions computed for  $n = 4$  in the right most column, and this is what limits the terminal state fidelity.

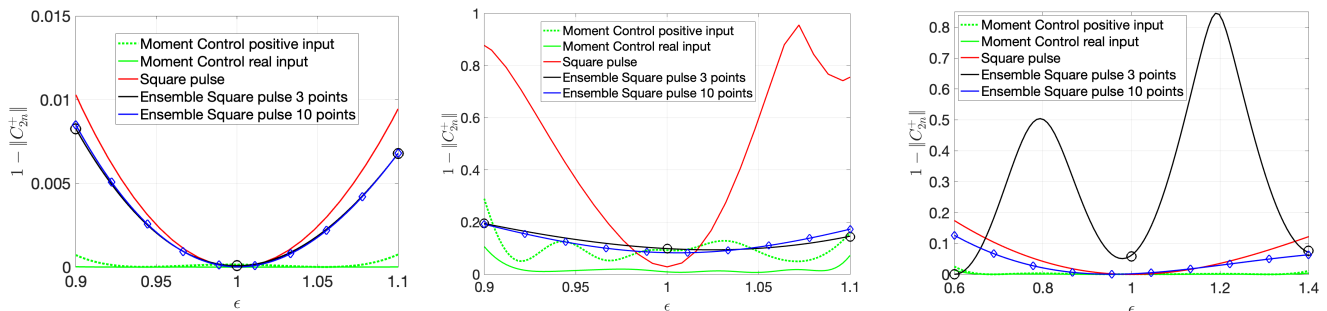


Fig. 3: Comparison of control performance, including the expanded square pulse design method for a collection of systems. The plots represent the design parameters (from left to right):  $\delta = 0.1$  and  $n = 1$ ;  $\delta = 0.1$  and  $n = 4$ ; and  $\delta = 0.4$  and  $n = 1$ .

using multiple  $\epsilon_i$  samples for  $i = 1, \dots, m$  are given in Table IV. The results for these scenarios are shown in Figure 3, and the values of the performance index  $I_e$  for the compared controls are shown in Table V. The table includes values  $I_{e,sp}$ ,  $I_{e,+}$ ,  $I_{e,\mathbb{R}}$ ,  $I_{e,3}$ , and  $I_{e,10}$  for the nominal parameter square pulse, the positive ensemble control, the real-valued ensemble control, the square pulse with  $m = 3$  samples, and the square pulse with  $m = 10$  samples, respectively, for all three control design cases described above.

The results show the limitations of the square pulse design, even when multiple samples are used over the ensemble parameter domain. For the first case shown at left in Figure 3, the ensemble square pulse approach (Problem (8)) provides little improvement in relation to the nominal square pulse (Problem (7)). The few degrees of freedom of the method

TABLE IV: Ensemble Square pulse design parameters.

$n$	$\delta$	$m$	$\Omega_1/\omega_r$	$\Omega_2/\omega_r$	$\omega_r\tau_1$	$\omega_r\tau_2$	$\omega_r\tau_3$
1	0.1	3	4.6404	4.2278	0.1943	0.9618	0.5286
1	0.4	3	10.6354	6.6525	1.2038	3.5000	0.5420
4	0.1	3	64.3286	27.5580	0.0924	3.4724	0.6647
1	0.1	10	4.0446	4.2140	0.3769	0.6386	0.6767
1	0.4	10	60.0000	4.6034	0.0159	2.6005	0.5322
4	0.1	10	60.8008	30.2755	0.0967	3.4694	0.6798

and the small domain  $K$  limits the improvement gained by sampling in the ensemble space. In the second and third cases, however, the improvement over using only one nominal value of  $\epsilon$  is noticeable. Nonetheless, the ensemble moment method exhibits significant improvements over the square pulse designs based on sampling.

TABLE V: Performance results for the computations including the ensemble square pulse approach.

$n$	$\delta$	$I_{e,sp}$	$I_{e,+}$	$I_{e,\mathbb{R}}$	$I_{e,3}$	$I_{e,10}$
1	0.1	0.0141	0.0021	0.0004	0.0127	0.0125
4	0.1	0.1768	0.0608	0.0260	0.0984	0.0965
1	0.4	0.2278	0.0030	0.0006	0.5884	0.1818

We conclude that directly sampling the ensemble parameter space  $K$  for the optimal control problem is not an effective means to compensate for inhomogeneities in the experimental setting. In contrast, the proposed ensemble control method promises to achieve improved and homogeneous performance for an entire BEC ensemble in a matter wave interferometry experiment.

## VI. CONCLUSION

We present a method for designing constrained optical pulses for optimal matter-wave splitting of a Bose-Einstein condensate in the presence of experimental inhomogeneities, which induce a parameter uncertainty within the momentum evolution of the collection of atoms. An ensemble of systems is parameterized by the factor that modulates the optical pulse, and Legendre moments are used to represent the optimal control problem for an infinite dimensional system as an optimization problem in moment space. The results demonstrate that the fidelity achieved by the proposed method has advantages over recently developed state-of-the-art optical pulse sequences. In particular, the method achieves precise momentum transfer of the BEC to high diffraction orders with inherent robustness to inhomogeneity in the effect of the optical pulse on atoms in the sample, and yields continuously-varying pulses that can be tuned to maximize the effectiveness of equipment in experimental settings.

We expect that future research will extend our results to more detailed models of BEC-splitting, as well as control protocols for additional experimental steps for state preparation and measurement. The moment method can be extended to incorporate more parameters to improve robustness to additional sources of uncertainty and inhomogeneity. Our computational approach could be improved and further analyzed to characterize the trade-offs in this setting between truncations in the moment and quantum Hilbert spaces, constraint bound values, pulse duration, and control performance. Based on the successful validation of our approach in simulation, we expect that optimal pulses can be tested in experimental settings to confirm anticipated improvements in performance of matter-wave diffraction metrology.

## REFERENCES

[1] Christiane P. Koch, Ugo Boscain, Tommaso Calarco, Gunther Dirr, Stefan Filipp, Steffen J. Glaser, Ronnie Kosloff, Simone Montangero, Thomas Schulte-Herbrüggen, Dominique Sugny, et al. Quantum optimal control in quantum technologies. strategic report on current status, visions and goals for research in europe. *EPJ Quantum Technology*, 9(1):19, 2022.

[2] Mary Clare Cassidy, Malcolm G Boshier, and Lee E Harrell. Improved optical standing-wave beam splitters for dilute Bose-Einstein condensates. *Journal of Applied Physics*, 130(19), 2021.

[3] B. Canuel, F. Leduc, D. Holleville, Alexandre Gauguet, J. Fils, A. Viridis, A. Clairon, N. Dimarcq, Ch J. Bordé, A. Landragin, et al. Six-axis inertial sensor using cold-atom interferometry. *Physical Review Letters*, 97(1):010402, 2006.

[4] P. A. Altin, M. T. Johnsson, Vladimir Negnevitsky, G. R. Dennis, Russell Paul Anderson, J. E. Debs, S. S. Szigeti, K. S. Hardman, Shayne Bennetts, G. D. McDonald, et al. Precision atomic gravimeter based on bragg diffraction. *New Journal of Physics*, 15(2):023009, 2013.

[5] Matt Jaffe, Victoria Xu, Philipp Haslinger, Holger Müller, and Paul Hamilton. Efficient adiabatic spin-dependent kicks in an atom interferometer. *Physical Review Letters*, 121(4):040402, 2018.

[6] Alexander Dunning, Rachel Gregory, James Bateman, Nathan Cooper, Matthew Himsforth, Jonathan A Jones, and Tim Freearge. Composite pulses for interferometry in a thermal cold atom cloud. *Physical Review A*, 90(3):033608, 2014.

[7] Jack Saywell, Max Carey, Mohammad Belal, Ilya Kuprov, and Tim Freearge. Optimal control of Raman pulse sequences for atom interferometry. *Journal of Physics B: Atomic, Molecular and Optical Physics*, 53(8):085006, 2020.

[8] Jr-Shin Li and Navin Khaneja. Control of inhomogeneous quantum ensembles. *Physical review A*, 73(3):030302, 2006.

[9] Shen Zeng and Frank Allgoewer. A moment-based approach to ensemble controllability of linear systems. *Systems & Control Letters*, 98:49–56, 2016.

[10] Yao-Chi Yu, Vignesh Narayanan, ShiNung Ching, and Jr-Shin Li. Learning to control neurons using aggregated measurements. In *2020 American Control Conference (ACC)*, pages 4028–4033. IEEE, 2020.

[11] Zaki Leghtas, Alain Sarlette, and Pierre Rouchon. Adiabatic passage and ensemble control of quantum systems. *Journal of Physics B: Atomic, Molecular and Optical Physics*, 44(15):154017, 2011.

[12] Anatoly Zlotnik, Raphael Nagao, István Z Kiss, and Jr-Shin Li. Phase-selective entrainment of nonlinear oscillator ensembles. *Nature communications*, 7(1):10788, 2016.

[13] Jr-Shin Li and Navin Khaneja. Ensemble control of bloch equations. *IEEE Transactions on Automatic Control*, 54(3):528–536, 2009.

[14] Xin Ning, André Luiz P. de Lima, and Jr-Shin Li. NMR pulse design using moment dynamical systems. In *IEEE 61st Conference on Decision and Control (CDC)*, pages 5167–5172, 2022.

[15] Saijun Wu, Ying-Ju Wang, Quentin Diot, and Mara Prentiss. Splitting matter waves using an optimized standing-wave light-pulse sequence. *Physical Review A*, 71(4):043602, 2005.

[16] Anatoly Zlotnik and Shin Li. Iterative ensemble control synthesis for bilinear systems. In *51st IEEE Conference on Decision and Control (CDC)*, pages 3484–3489. IEEE, 2012.

[17] Vignesh Narayanan, Wei Zhang, and Jr-Shin Li. Moment-based ensemble control. *arXiv preprint arXiv:2009.02646*, 2020.

[18] Jr-Shin Li, Wei Zhang, and Yuan-Hung Kuan. Moment quantization of inhomogeneous spin ensembles. *Annual Reviews in Control*, 54:305–313, 2022.

[19] Alexander D. Cronin, Jörg Schmiedmayer, and David E. Pritchard. Optics and interferometry with atoms and molecules. *Reviews of Modern Physics*, 81(3):1051, 2009.

[20] Wei Xiong, Xuguang Yue, Zhongkai Wang, Xiaoji Zhou, and Xuzong Chen. Manipulating the momentum state of a condensate by sequences of standing-wave pulses. *Physical Review A*, 84(4):043616, 2011.

[21] Yao-Chi Yu, Vignesh Narayanan, and Jr-Shin Li. Moment-based reinforcement learning for ensemble control. *IEEE Transactions on Neural Networks and Learning Systems*, pages 1–12, 2023.

[22] Shen Zeng. Iterative optimal control syntheses illustrated on the Brockett integrator. *IFAC-PapersOnLine*, 52(16):138–143, 2019.

[23] Minh Vu and Shen Zeng. Iterative optimal control syntheses for nonlinear systems in constrained environments. In *2020 American Control Conference (ACC)*, pages 1731–1736. IEEE, 2020.